



## Direct measurement and analysis of the conduction band density of states in diluted $\text{GaAs}_{1-x}\text{N}_x$ alloys

L. Ivanova,<sup>1</sup> H. Eisele,<sup>1,\*</sup> M. P. Vaughan,<sup>2</sup> Ph. Ebert,<sup>3</sup> A. Lenz,<sup>1</sup> R. Timm,<sup>1</sup> O. Schumann,<sup>4,5</sup> L. Geelhaar,<sup>4,6</sup> M. Dähne,<sup>1</sup> S. Fahy,<sup>2,7</sup> H. Riechert,<sup>4,6</sup> and E. P. O'Reilly<sup>2</sup>

<sup>1</sup>*Institut für Festkörperphysik, Technische Universität Berlin, Hardenbergstraße 36, 10623 Berlin, Germany*

<sup>2</sup>*Tyndall National Institute, Lee Maltings, Cork, Ireland*

<sup>3</sup>*Institut für Festkörperforschung, Forschungszentrum Jülich GmbH, 52425 Jülich, Germany*

<sup>4</sup>*Infineon Technologies AG, 81730 München, Germany*

<sup>5</sup>*Carl Zeiss SMT AG, 73447 Oberkochen, Germany<sup>†</sup>*

<sup>6</sup>*Paul-Drude-Institut für Festkörperelektronik, Hausvogteiplatz 5-7, 10117 Berlin, Germany<sup>‡</sup>*

<sup>7</sup>*Department of Physics, University College Cork, Cork, Ireland*

(Received 14 September 2010; published 7 October 2010)

We use scanning tunneling spectroscopy to show directly that the conduction band density of states (DOS) of  $\text{GaAs}_{1-x}\text{N}_x$  with low nitrogen (N) content  $x$  is enhanced about 0.5 eV above the band edge, followed by a decrease at higher energy. The structure of the measured DOS is in excellent agreement with calculations based on a Green's-function formalism taking into account different N environments. This analysis highlights the inclusion of N-N pairs and the validity of the Green's-function approach to describe the band structure of dilute nitride and related extreme semiconductor alloys.

DOI: [10.1103/PhysRevB.82.161201](https://doi.org/10.1103/PhysRevB.82.161201)

PACS number(s): 71.20.Nr, 71.23.An, 68.37.Ef, 71.55.Eq

There has been considerable interest concerning extreme, or highly mismatched, semiconductor alloys, which are characterized by large differences in covalent radii and/or electronegativity between the alloying species, placing them beyond the assumptions of the virtual-crystal approximation used in the modeling of conventional alloys. An archetypal example of these alloys are dilute nitrides, i.e., dilute concentrations of nitrogen (N) in GaAs and  $\text{In}_y\text{Ga}_{1-y}\text{As}$ . It is now well established that N forms a resonant defect level above the conduction band (CB) in GaAs and gives rise to a profound bowing of the band gap with increasing concentration.<sup>1</sup>

The band anticrossing (BAC) model<sup>2</sup> has provided a simple but useful explanation of the band-gap bowing in terms of a hybridization between the localized N states and the extended states of the host semiconductor. According to this model, the CB splits into upper and lower bands ( $E_+$  and  $E_-$ ) with the lower band ( $E_-$ ) becoming highly nonparabolic and flattening out in  $k$  space as it approaches the N energy level. Despite evidence for this restructuring of the CB,<sup>3,4</sup> the nature of the CB dispersion relation near the N energy level remains unclear.

An intrinsic problem of the BAC model is an unphysical prediction of an infinite number of states below any given N level. This arises from the density of states (DOS) derived from the predicted dispersion relations being nonintegrable as the N level is approached. A possible solution to this problem is the derivation of the BAC model<sup>5</sup> from a single-impurity Anderson model.<sup>6</sup> This approach introduces an imaginary component of the N energy, interpreted as a homogeneous or lifetime broadening. A well-defined DOS can then be derived from the imaginary part of the Green's function of the system. This method has subsequently been extended to the many-impurity case,<sup>7</sup> allowing the formal modeling of different N environments. However, neither the energies of these environments, and hence the *inhomoge-*

*neous* broadening of the states in energy, nor the hybridization strengths are currently derived from the model.

Deeper theoretical investigations into the band structure of dilute nitrides have followed complementary paths. On the one hand, calculations based on the empirical pseudopotential method (EPM) (Ref. 8) emphasize a picture away from hybridization and explain the restructuring of the CB edge in terms of the mixing of X and L valleys in the Brillouin zone via the N potential. Moreover, EPM calculations suggest that the CB edge has a far higher degree of localization than suggested by the BAC model while finding no evidence for the formation of the upper  $E_+$  band. On the other hand, tight-binding calculations offer more direct support for the BAC model interpretation.<sup>9</sup> This tight-binding approach allows a basis of extended states and a linear combination of isolated N states (LCINS) to be extracted from the full Hamiltonian of the system.<sup>10</sup> The interaction between different N states is naturally incorporated in this model and gives quantitative predictions of the energy levels and hybridization strengths in isolated N different environments as well as for local N clusters. The LCINS approach has already been successful in explaining the anomalous N concentration dependence of the band-edge effective mass<sup>11</sup> and has been used to calculate mobility in conjunction with a model of resonant scattering.<sup>12</sup>

More recently, attention has been focused on the high-field electronic properties of dilute nitrides. The extreme nonparabolicity of the CB led to the suggestion that these materials may exhibit a negative differential resistance at high fields, as indeed observed for dilute  $\text{GaAs}_{1-x}\text{N}_x$ ,<sup>13</sup> and opens up possibilities for microwave or even terahertz applications. Dilute nitrides could be a good candidate material for avalanche photodetectors,<sup>14</sup> where the degradation in electron mobility actually becomes advantageous. This reduces the electron ionization coefficient relative to that of holes, leading to a more stable device with a lower noise

factor. Such applications will depend crucially on the true nature of the CB states as one moves up in energy toward the N energy level and possible transmission to the higher mobility band above.

In the present work, the DOS in a dilute nitride  $\text{GaAs}_{1-x}\text{N}_x$  sample as the archetypal example of such alloys is determined experimentally using cross-sectional scanning tunneling spectroscopy (XSTS). The measured DOS is modeled theoretically using the Green's-function framework in conjunction with LCINS calculations for the energy levels and hybridization strengths of the different N environments. Using the Green's-function model for a single impurity alone qualitatively reproduces the observed trends in the DOS near the N energy level but requires an arbitrary broadening far in excess of the predicted homogeneous broadening to fit the data. Incorporating disorder by using the calculated LCINS energy parameters removes this arbitrariness and produces an excellent fit to the experimental data while allowing us to identify observed features in the spectra associated with particular N environments. These environments are observed directly via cross-sectional scanning tunneling microscopy (XSTM), confirming the random distribution of N sites assumed in the LCINS model.

For the XSTS and XSTM investigations we used a 15-nm-thick layer of  $\text{GaAs}_{1-x}\text{N}_x$  with a nominal N concentration of  $x=0.012$  within a pure GaAs matrix, grown by molecular-beam epitaxy as described in Refs. 15 and 16. Such a thick  $\text{GaAs}_{1-x}\text{N}_x$  layer can be assumed to exhibit bulklike behavior. Two-dimensional effects can be neglected, except a small biaxial strain with respect to the underlying GaAs lattice of  $-0.25\%$ . The XSTM and XSTS measurements were performed using a home-built microscope with an RHK SPM 1000 control unit. Electrochemically etched tungsten tips cleaned *in situ* by electron bombardment were used. The samples were cleaved along the (110) crystal plane in ultra-high vacuum ( $p < 10^{-8}$  Pa).

Figure 1(a) shows an overview filled-state XSTM image of the  $\text{GaAs}_{1-x}\text{N}_x$  layer acquired at a sample voltage  $V=-2.5$  V. At this polarity, the bright lines along  $[\bar{1}10]$  direction represent the filled dangling bonds of topmost arsenic (As) atoms of the GaAs(110) surface.<sup>17,18</sup> In addition, dark spots of the size of one atom can be observed within the As rows [marked by gray (yellow) circles]. Figure 1(c) shows a high-resolution XSTM image of such a dark spot. A height profile across such a dark spot [taken along the (red) dashed line in Fig. 1(c)] shows the presence of a filled dangling bond at this arsenic lattice site, as shown in Fig. 1(d). The presence of such a dangling bond is consistent with an N atom, being inward relaxed due to its shorter backbonds, in agreement with theoretical *ab initio* calculations.<sup>19</sup> This appearance of N atoms in the topmost layer of the GaAs(110) surface provides a distinction from As vacancies,<sup>20</sup> which also appear as dark spots but at which no dangling bond is present [blue line in Fig. 1(d)]. The dark spots with the inward relaxed dangling bonds were counted directly from the XSTM images<sup>16</sup> and their average concentration was determined to  $(1.2 \pm 0.1)\%$ . This concentration is in excellent agreement with the nominal N concentration, corroborating the above identification of the individual N atoms in accordance with Refs. 16 and 21.

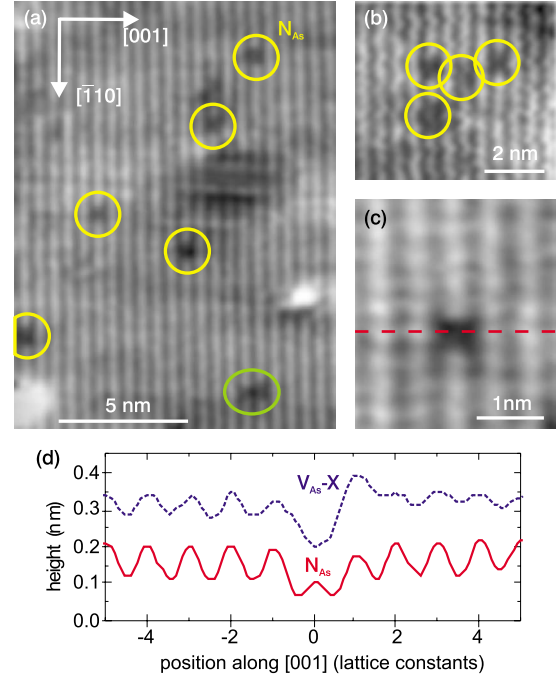


FIG. 1. (Color online) (a) Filled-state overview XSTM image of the  $\text{GaAs}_{1-x}\text{N}_x$  layer with  $x=0.012$ , measured at  $V=-2.5$  V and  $I=140$  pA. Single N atoms in the topmost layer of the GaAs(110) surface are indicated by gray (yellow) circles. The gray (green) ellipse highlights two N atoms in adjacent atomic rows. (b) Filled-state XSTM image of an agglomeration of N atoms, measured at  $V=-2.5$  V and  $I=140$  pA. (c) High-resolution image of one single N atom, measured at  $V=-3.7$  V and  $I=88$  pA. (d) Height profile of the GaAs(110) surface with a single N atom at an arsenic lattice site ( $N_{As}$ ) [(red) solid line], measured along the (red) dashed line in (c). Note the presence of a dangling bond at the N related position (0). For comparison, a profile through an arsenic vacancy-defect complex ( $V_{As}-X$ ) at the (110) surface of a GaAs substrate is shown as (blue) dashed line. The anion-related dangling bond is missing.

The N atoms were not found to be homogeneously distributed. Occasionally, local pairs of N atoms in neighboring atomic rows occur [gray (green) ellipse in Fig. 1(a)]. In addition, also larger agglomerations of N atoms occur, as visible in Fig. 1(b). Although only every second (001) plane appears as an atomic row in XSTM images of zinc-blende (110) surfaces,<sup>17</sup> these observations indicate the existence of close neighbor N pairs and other agglomerations.

In the layer shown in Fig. 1(a), current-voltage spectra ( $I$ - $V$ ) as well as differential conductance-voltage spectra  $[(dI/dV)-V]$  were measured using the variable gap mode.<sup>22</sup> From this data the normalized differential conductance  $(dI/dV)/(I/V)$  is determined,<sup>23</sup> which is approximately proportional to the local DOS (LDOS). The resulting normalized differential conductance spectrum as a function of voltage or corresponding energy is shown as blue circles in Fig. 2. As a reference,  $(dI/dV)/(I/V)$  were also taken at the GaAs layers beside the 1.2% N containing layer. During growth of these layers the radio-frequency nitrogen plasma source was already burning, resulting in an ultradilute N contamination of the GaAs even if the shutter in front of the plasma source is closed. In accordance to this, in these layers we could

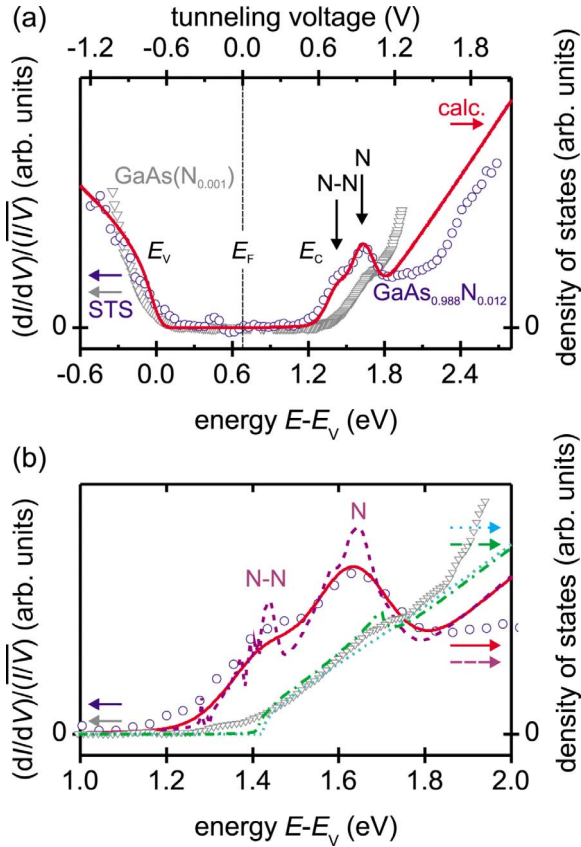


FIG. 2. (Color online) (a) Normalized differential conductance  $(dI/dV)/(I/V)$  spectrum of  $\text{GaAs}_{0.988}\text{N}_{0.012}$  [(blue) circles, left and top axes]. DOS calculated using the LCINS model for  $x=0.012$  with extrinsic thermal and modulation broadening incorporated [(red) solid line, marked calc., right and bottom axes]. (b) Same as (a) but magnified to highlight the conduction band states. In addition, the (purple) dashed line shows the calculated DOS without the extrinsic broadening. The peaks in the differential conductance spectrum in (a) (marked by black arrows) correspond with the states arising from single N atoms (N) and pairs of N atoms (N-N) in the DOS in (b). For comparison the  $(dI/dV)/(I/V)$  spectrum of  $\text{GaAs}(\text{N}_{0.001})$  is shown [(gray) triangles], in (b) together with the unbroadened calculated DOS for pure GaAs [(cyan) dotted line] and 0.1% N containing GaAs [(green) dashed-dotted line].

observe an N content of about 0.1%.<sup>16</sup> One  $I$ - $V$  spectrum taken at such a region is also shown in Fig. 2 [ $\text{GaAs}(\text{N}_{0.001})$ , (gray) triangles] as reference.

The measured normalized differential conductance spectrum exhibits a clear band gap between the valence band (VB) maximum ( $E_V \equiv 0$  eV) and the conduction band minimum ( $E_C$ ). This band gap is about 1.2 eV wide, i.e., about 0.25 eV smaller than the fundamental band gap of GaAs (1.43 eV at  $T=300$  K). Moreover, two additional signatures above  $E_C$  at energetic positions of about 1.4 and 1.6 eV are visible in the spectrum, as marked by black arrows. Furthermore, between energies of about 1.8 and 2.3 eV a reduced but nonzero differential conductance is observed. This observation is not in agreement with a second band gap, as would result from the BAC model between  $E_V+1.6$  and  $E_V+1.8$  eV. Finally, the Fermi energy is approximately in the midgap position ( $E_F=E_V+0.68$  eV), in accordance with the

intrinsic conditions between the  $n$ - and  $p$ -doped cladding layer below and above the N containing layer, respectively. In contrast to these findings, the  $\text{GaAs}(\text{N}_{0.001})$  spectrum exhibits a band gap of about 1.4 eV and does not show comparable signatures in the conduction band while at the valence band its behavior is very similar to the N containing spectrum. Its spectral characteristics up to 2.0 eV are in good agreement with  $(dI/dV)/(I/V)$  spectra measured on pure GaAs.<sup>24</sup>

In order to describe the measured differential conductance spectra, in principle, the Green's-function formalism may be used alone, assuming an arbitrary broadening on the localized N state energy. However, here a more fundamental approach is taken, using the LCINS model, which gives a distribution of N state energies due to their mutual interaction. LCINS state energies and interaction energies as calculated in Ref. 12 were used directly in Eqs. (21) and (22) of Ref. 7 to calculate the perturbed DOS without arbitrarily fitting the energy broadening. The nonparabolic GaAs CB parameters were taken from Ref. 25.

The (purple) dashed line in Fig. 2(b) shows the calculated DOS of the lower portion of the CB as derived from the LCINS model. We see that the calculated DOS displays a detailed structure, which we can identify with particular types of N environments. The main signature is a peak around  $E_V+1.65$  eV corresponding to energy states of isolated N atoms. In addition, a series of smaller peaks around  $E_V+1.4$  eV is related to states from N-N pairs. These peaks are not present in the reference data from the  $\text{GaAs}(\text{N}_{0.001})$  region, where only a tiny plateau is visible at about 1.7 eV. This plateau might be related to the small peak in the calculated (unbroadened) DOS for 0.1% of N [(green) dashed-dotted line]. Over all, the measured  $(dI/dV)/(I/V)$  spectrum is in good agreement with the two almost similar calculated DOS for pure and 0.1% N containing GaAs.

An important point to note is that the calculated DOS shown here results due to the projection of the perturbed states onto the  $\mathbf{k}$  states of GaAs. In other words, the local DOS associated with the isolated N states is excluded. In bulk  $\text{GaAs}_{0.998}\text{N}_{0.012}$ , the DOS projected onto these states would be very large in comparison to that projected onto the GaAs host matrix  $\mathbf{k}$  states, and should dominate the measured data. However, it can be observed from Fig. 1 that N atoms on the surface can relax away from the tetrahedral configuration, and it is known that N atoms in the second and third layer below the (110) surface do also relax.<sup>26</sup> This should eliminate the N resonant states at or near the surface, in a similar fashion to hydrogen passivation of N in hydrogenated samples.<sup>27</sup> Since the N states are highly localized, they are therefore not probed directly by surface spectroscopy and so do not contribute to the measured LDOS.

In addition to the broadening effects intrinsic to the material as described above, the differential conductance spectrum also exhibits extrinsic broadening effects due to the experimental procedure. On the one hand a thermal broadening occurs due to the finite temperature at which the measurements are carried out. The thermal broadening is given by the full width at half maximum of the derivative of the *Fermi-Dirac* distribution  $\Delta E_{\text{th}} = 2k_B T \ln(3+2\sqrt{2}) = 91$  meV at  $T=300$  K. On the other hand, a modulation broadening



arises due to sampling the tunneling voltage (which corresponds to the energy) for lock-in detection.

The (red) solid lines in Figs. 2(a) and 2(b) show the calculated DOS subjected to this extrinsic (experimental) broadening. Note that the energy reference is imposed only by the requirement that the VB edge  $E_V$  lines up with the differential conductance data. Except for the scale of the DOS, no fitting parameter is used.

Using the LCINS data and folding in the extrinsic broadening, the calculated DOS is in good agreement with the experimental differential conductance data. In particular, the width of the band gap, the N related peaks, and the DOS reduction above are found at the same energies in both the experimental measurement as well as the calculation. The main physical aspect to achieve this good agreement is taking into account of states due to the N-N pairs. This results in the shoulder in the spectrum at about  $E_V + 1.4$  eV for this particular N concentration. This highlights that the N-N pairs and also other agglomerations observed in the XSTM images in Fig. 1 directly affect the electronic states already for a N concentration of  $x=0.012$ . In extremely diluted N containing GaAs, where the presence of N-N pairs is negligible, this shoulder should vanish. In contrast, for extremely high N containing GaAs, the intermixing of the N-N pairs and further agglomerations is expected to become dominant in the

differential conductance spectra of the CB without exhibiting any distinctive peak, in agreement with XSTS measurements.<sup>28</sup> Nevertheless, as long as the N concentration is sufficiently small that instead of a continuous band the DOS is dominated by states of single N and N-N pairs, the DOS above these states is reduced but always remains at a nonzero value.

In conclusion, we have determined the density of states in dilute  $\text{GaAs}_{1-x}\text{N}_x$  with a N concentration of  $x=0.012$ , finding experimental evidence, beyond the ultradilute limit, for the restructuring of the higher-lying conduction band states. We have shown that incorporating LCINS calculations into the Green's-function formalism yields an excellent explanation of the observed data without arbitrary fitting parameters and allows us to identify signatures in the energy spectra with localized N environments, particularly the single N and N-N pair related states. The success of this approach provides direct confirmation for the hybridization picture of dilute nitrides, and should prove a useful starting point in the investigation of other extreme alloys.

This work was supported by the German Science Foundation DFG, collaborative research center Sfb 787 TP A4 and project Ei 788/1-1, as well as by the Science Foundation Ireland.

\*ak@physik.tu-berlin.de

†Present address.

- <sup>1</sup>M. Weyers, M. Sato, and H. Ando, *Jpn. J. Appl. Phys., Part 2* **31**, L853 (1992).
- <sup>2</sup>W. Shan, W. Walukiewicz, J. W. Ager, III, E. E. Haller, J. F. Geisz, D. J. Friedman, J. M. Olson, and S. R. Kurtz, *Phys. Rev. Lett.* **82**, 1221 (1999).
- <sup>3</sup>J. Endicott, A. Patanè, J. Ibáñez, L. Eaves, M. Bissiri, M. Hopkinson, R. Airey, and G. Hill, *Phys. Rev. Lett.* **91**, 126802 (2003).
- <sup>4</sup>A. Patanè, J. Endicott, J. Ibáñez, P. N. Brunkov, L. Eaves, S. B. Healy, A. Lindsay, E. P. O'Reilly, and M. Hopkinson, *Phys. Rev. B* **71**, 195307 (2005).
- <sup>5</sup>J. Wu, W. Walukiewicz, and E. E. Haller, *Phys. Rev. B* **65**, 233210 (2002).
- <sup>6</sup>P. W. Anderson, *Phys. Rev.* **124**, 41 (1961).
- <sup>7</sup>M. P. Vaughan and B. K. Ridley, *Phys. Rev. B* **75**, 195205 (2007).
- <sup>8</sup>P. R. C. Kent, L. Bellaiche, and A. Zunger, *Semicond. Sci. Technol.* **17**, 851 (2002).
- <sup>9</sup>E. P. O'Reilly *et al.*, *Semicond. Sci. Technol.* **17**, 870 (2002).
- <sup>10</sup>A. Lindsay and E. P. O'Reilly, *Phys. Rev. Lett.* **93**, 196402 (2004).
- <sup>11</sup>F. Masia *et al.*, *Phys. Rev. B* **73**, 073201 (2006).
- <sup>12</sup>S. Fahy, A. Lindsay, H. Ouerdane, and E. P. O'Reilly, *Phys. Rev. B* **74**, 035203 (2006).
- <sup>13</sup>A. Patanè, A. Ignatov, D. Fowler, O. Makarovskiy, L. Eaves, L. Geelhaar, and H. Riechert, *Phys. Rev. B* **72**, 033312 (2005).
- <sup>14</sup>A. R. Adams, *Electron. Lett.* **40**, 1086 (2004).
- <sup>15</sup>O. Schumann, S. Birner, M. Baudach, L. Geelhaar, H. Eisele, L. Ivanova, R. Timm, A. Lenz, S. K. Becker, M. Povolotskiy, M. Dähne, G. Abstreiter, and H. Riechert, *Phys. Rev. B* **71**, 245316 (2005).
- <sup>16</sup>L. Ivanova *et al.*, *Appl. Phys. Lett.* **92**, 203101 (2008).
- <sup>17</sup>R. M. Feenstra, J. A. Stroscio, J. Tersoff, and A. P. Fein, *Phys. Rev. Lett.* **58**, 1192 (1987).
- <sup>18</sup>N. D. Jäger, E. R. Weber, K. Urban, and Ph. Ebert, *Phys. Rev. B* **67**, 165327 (2003).
- <sup>19</sup>H. Abu-Farsakh and J. Neugebauer (private communication).
- <sup>20</sup>Ph. Ebert, K. Urban, L. Aballe, C. H. Chen, K. Horn, G. Schwarz, J. Neugebauer, and M. Scheffler, *Phys. Rev. Lett.* **84**, 5816 (2000), and references therein.
- <sup>21</sup>H. A. McKay *et al.*, *J. Vac. Sci. Technol. B* **19**, 1644 (2001).
- <sup>22</sup>R. M. Feenstra, *Phys. Rev. B* **50**, 4561 (1994). We used a tip-height change  $\Delta z/\Delta V$  of 1.5 Å/V, a lock-in oscillator frequency of 10 kHz, and an effective oscillator amplitude of 40 mV.
- <sup>23</sup>M. Prietsch, A. Samsavar, and R. Ludeke, *Phys. Rev. B* **43**, 11850 (1991); L. Ivanova *et al.*, *Appl. Phys. Lett.* **93**, 192110 (2008) using  $(I/V) = \sqrt{(I/V)^2 + c^2}$  with  $c=50$  pA/V.
- <sup>24</sup>R. M. Feenstra and P. Mårtensson, *Phys. Rev. Lett.* **61**, 447 (1988).
- <sup>25</sup>I. Vurgaftman, J. R. Meyer, and L. R. Ram-Mohan, *J. Appl. Phys.* **89**, 5815 (2001).
- <sup>26</sup>H. A. McKay *et al.*, *Appl. Phys. Lett.* **78**, 82 (2001).
- <sup>27</sup>G. Baldassarri H. v. H. *et al.*, *Appl. Phys. Lett.* **78**, 3472 (2001).
- <sup>28</sup>R. S. Goldman *et al.*, *Appl. Phys. Lett.* **69**, 3698 (1996).